Surface phonons on the (001) surface of a fcc crystal covered with a $C(2\times2)$ monolayer

G. Armand

Section d'Etudes des interactions gaz-solide, Service de Physique Atomique-Bâtiment 62-Centre d'Etudes Nucléaires de Saclay, B.P. No. 2-91190 Gif sur Yvette, France

J. B. Theeten

Laboratoires d'Electronique et de Physique appliquée, B.P. 15-94450 Limeil Brevannes, France

(Received 9 October 1973)

We present here a calculation of the energies and the polarizations of the surface phonons in a realistic case: a (001) surface of a fcc crystal covered with a $C(2\times2)$ monolayer [experimental case of Ni(100)+S$C(2\times2)$ for instance]. The method, derived from a former calculation by Gazis and Wallis on the clean (001) surface of a bcc crystal, is applied to any type of $C(2\times2)$ monolayer: reconstructed, nonreconstructed, and $P(1\times1)$ structure. The results are given for the waves propagating in the [100] direction. A correspondence between the spectra of the $P(1\times1)$ and reconstructed $C(2\times2)$ structures is demonstrated. For $C(2\times2)$ structures, the low-wave-vector phonons depend mainly on the bonds between adsorbate and substrate atoms. The high-wave-vector phonons depend, in addition, on the bonds between the adsorbate atoms. In particular, a clear-cut test is provided for deciding between the reconstructed and nonreconstructed $C(2\times2)$ structures.

I. INTRODUCTION

Important improvements have been recently obtained in the knowledge of the vibrational properties of the surfaces, both in the experimental and theoretical fields. Infrared absorption spectroscopy, long used for determining the vibrational frequencies of various species adsorbed on substrates exhibiting an important surface-volume ratio, has been extended to the cases of monocrystalline[1] and polycrystalline[2] substrates. Slow-electron-loss spectroscopy has been successfully applied to the clean surfaces of ZnO (0001) and Si (111),[3] and to some adsorbed monolayers.[4] Very recently, the analysis of the scattering of helium atoms of thermal energy has allowed to determine the dispersion curve of the Rayleigh-type surface phonons on LiF (100).[5] Furthermore, the low-energy-electron-diffraction (LEED) technique and theory are now sufficiently developed to determine the crystalline structure of an adsorbed monolayer in simple cases.[6] Experimental techniques are thus available for measuring the characteristics of the surface phonons in the case of an adsorbed monolayer.

Theoretical work on this subject has been mostly devoted, up until now, to the case of a $P(1\times1)$ adsorbed monolayer. In this case, the adsorbed monolayer has the same crystalline structure as the uppermost layer of the substrate. One can vary the mass of the adsorbed atoms[7-10] or the force constants between adsorbed and substrate atoms.[11] Various crystalline structures for the substrate have been investigated: (i) simple cubic with central forces between first and second neighbors[7] and angular forces between first neighbors[8]; (ii) body-centered cubic with the same types of forces[9]; and (iii) face-centered cubic with the same types of forces[11] or Lennard-Jones-type interaction.[10]

The method used for the calculations is generally a perturbation method which implies the calculation of the matrix elements of the Green's function for the clean surface. A complete analytic solution is possible only in the case of a simple cubic lattice.[7,8] In the other cases, the authors use either an expansion formula, only valid for high-frequency phonons,[9] or a direct numerical calculation.[10,11] In this last case, the crystal is reduced to a finite number of layers. Very recently, the general effects of a reconstruction of the surface plane on the optical surface phonons have been investigated.[12]

It then seems to be useful to proceed further to real experimental cases. One of the most simple real situation we intend to study here is that of an adsorbed monolayer in $C(2\times2)$ structure on the (001) surface of a face-centered-cubic crystal. A number of distinct situations are possible: the mass of a substrate atom; the force constants between adsorbed atoms and between adsorbed and substrate atoms can be different from the bulk force constants; the $C(2\times2)$ adsorbed layer can be either a monoatomic layer of foreign atoms [hereafter referred as a nonreconstructed $C(2\times2)$ layer and denoted $C(2\times2)$NR] or mixed layer of foreign and substrate atoms [hereafter refered as a reconstructed $C(2\times2)$ layer and denoted $C(2\times2)$R].

A comparison between experimental and theoretical results would allow to determine which situation is met for any given adsorbate-substrate system.

Since the Green's-function method cannot be used in a complete analytic way in this case (face-centered-cubic substrate), we have extended a method developed by Gazis and Wallis[13] in the case of a clean (001) face of a body-centered-cubic crystal. In this method, a displacement field is assumed, of the following form:

$$(u, v, w) = K(X, Y, Z) \exp[-qz + i(k_x x + k_y y - \omega t)],$$

which must be compatible with the atomic equations of motions in the bulk and at the surface. (z denotes the direction normal to the surface.) At a given set of k_x, k_y, and ω, the compatibility implies a certain value for q. If q is purely imaginary, the displacement field corresponds to a bulk wave. If $\exp(-q)$ is real positive (negative), the displacement field corresponds to a Rayleigh (alternating Rayleigh) wave. If q is complex, this corresponds to a generalized Rayleigh wave (the displacements are a product of a sinusoidal and a decaying exponential function). This method has the important advantage to give, in addition to the dispersion curves, the polarization and the attenuation factor of the surface waves.

In Sec. II, we will describe the model we have adopted for the crystalline structure and the force constants. In Sec. III, we discuss some general properties of the model. In Sec. IV, we develop the equation necessary for the calculation. The results and discussions are given in Sec. V.

II. DESCRIPTION OF THE MODEL

A. Crystalline structure

As already mentioned above, various types of $C(2\times2)$ adsorbed layers have been recognized experimentally.[14] We have then adopted for the crystalline structure of the surface, a very general model able to describe each particular system. In Fig. 1, we give a top view of the (001) surface of a fcc crystal covered with the most general type of a $C(2\times2)$ layer. The crystal atoms are arranged in a square lattice. On this lattice, two types of atoms, A and B, are adsorbed. The A atoms, for instance, because of their radius, cannot get closer to one another than building up a square lattice $\sqrt{2}\times\sqrt{2}$ greater than the crystal one, and rotated by 45°. This constitutes a $C(2\times2)$ lattice. The B atoms are inserted in the vacancies of the A lattice; this implies that they build up another $C(2\times2)$ lattice imbricated in first one. For sake of simplicity, the adsorbed layer is assumed to be planar, i.e., we assume the length of the bonds A–crystal and B–crystal to be equal. Furthermore, the distance $\frac{1}{2}d$ between the adsorbate plane ($n=0$) and the first substrate plane ($n=1$) is assumed to be equal to the spacing $\frac{1}{2}a$ between the substrate (001) planes. These translations of the atom positions from their actual ones, provided that they are small, are equivalent to a simple normalization of the force constants between the atoms in the $n=0$ and $n=1$ planes. As the adsorbate plane contains two distinct types of atoms, the atoms in the $n=1$ plane must be considered of two different types, C and D, defined by their different surroundings.

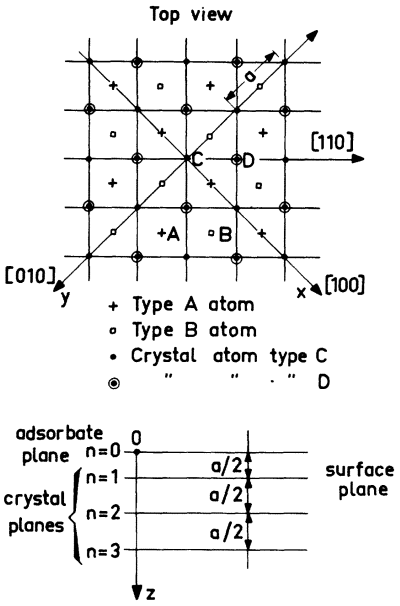

FIG. 1. Crystalline structure of the Ni(100) surface covered with the most general type of $C(2\times2)$ monolayer.

As can be seen in Fig. 1, we can describe each experimental situation by an appropriate choice of A and B atoms. If the B atoms are suppressed, we obtain a nonreconstructed adsorbed layer, denoted $C(2\times2)$NR: this is, for instance, the experimental case of Ni (100) + NaC(2×2).[6] If B atoms are crystal atoms, we obtain a reconstructed adsorbed layer, denoted $C(2\times2)$R: this is for instance, the experimental case of Ni (100) + OC ×(2×2).[15,16] Recently, King[17] has proposed a decomposition of the CO molecule in the W (100) + COC(2×2) system. If the same decomposition occurred on Ni (100) this would correspond to the case where A is a carbon and B is an oxygen. Finally, if we assume $A=B$, the adsorbate plane reduces to a $P(1\times1)$ lattice; this case is less frequently observed but it allows us to compare our results with previous work[7–11] and to better understand the effect of reconstruction on the surface phonons.[12]

The Brillouin zone corresponding to the crystalline structure of Fig. 1 is given in Fig. 2 where the projection of the bulk Brillouin zone on the (001) surface is compared to the $P(1\times1)$ and

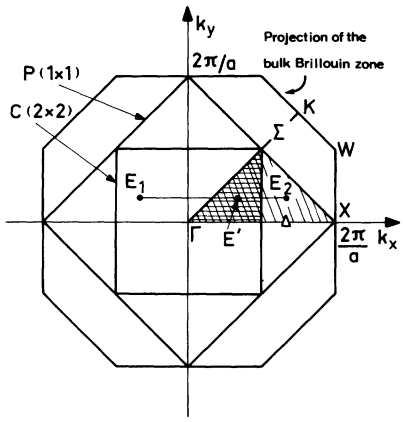

FIG. 2. Brillouin zones for the surface waves in the $P(1\times1)$ and $C(2\times2)$ cases compared with the projection of the bulk Brillouin zone. The hatched areas are the irreducible parts of these Brillouin zones.

$C(2\times2)$ Brillouin zones. The hatched areas are the irreducible parts of these Brillouin zones. This means that each surface mode in the $P(1\times1)$ case is obtained when its vector (k_x, k_y) is contained in the $\Gamma\Sigma X$ area. In the $C(2\times2)$ case, (k_x, k_y) can be restricted to the double-hatched area limited by ΓX, $\Gamma\Sigma$, and the $k_x=\pi/a$ axis. A general property of the surface modes in the two cases can be deduced from the symmetries of the Brillouin zones. If we consider the particular case where A atoms and B atoms are nearly identical, the $C(2\times2)$R structure tends to a $P(1\times1)$ structure. Each surface mode for the $P(1\times1)$ structure with a wave vector lying in the double-hatched area will be a surface mode for the $C(2\times2)$R structure with the same wave vector. Furthermore, for the $C(2\times2)$R structure, the points E_1, E', and E_2 are equivalent (E_1 and E_2 are deduced from each other through a reciprocal-lattice vector, E_1 and E' are symmetric with respect to the $k_x=0$ axis). Then, to each surface mode associated with E_2 will correspond a surface mode of the same energy associated with E'. As E' and E_2 are symmetric with respect to the $k_x=\pi/a$ axis, if we get n branches for the $P(1\times1)$ structure, the n branches deduced from the first ones by symmetry with respect to the $k_x=\pi/a$ axis will be also surface modes for the $C(2\times2)$R structure. In other words, if we obtain n branches for the $P(1\times1)$ structure, they will correspond to $2n$ branches for the $C(2\times2)$R structure. These $2n$ branches can remain surface modes but can also fall, through the symmetry, into bulk bands and become virtual surface modes. This point has already been noticed by Dobrzynski and Mills[12]; it will be extensively discussed further. For now, let us simply note that, as the $C(2\times2)$ Brillouin zone is half the size of the $P(1\times1)$ zone the total number of surface modes is the same in the two cases. This general property is independent of the type of interaction between atoms.

B. Force constants

By restriction to small atomic displacements, the interactions between the atoms can be described as harmonic potentials. The force constants of these harmonic potentials will constitute with the masses of A and B atoms the parameters of the calculation. We will restrict ourselves to the central-type interactions (in the sense of de Launay[18] between nearest neighbors. The approximation is necessary to limit the number of parameters [seven parameters in the $C(2\times2)$R case in this approximation, and at least nine in any further developed approximation]. On the other hand, this approximation can be quite valid for the bulk modes of nickel or copper crystals. In fact, the dispersion relations for the bulk phonons calculated in this approximation agree quite well with the experimental data obtained from inelastic neutron scattering, as already mentioned by Clark, Herman, and Wallis.[19] In the case of nickel, the central force constant α_{MM} between nearest-neighbor bulk atoms is adjusted in such a way that the experimental and calculated maximum frequencies coincide. For nickel $\alpha_{\mathrm{Ni\,Ni}}=3.79\times10^4$ dyn/cm. The comparison between theory and experiment[20] is illustrated in Figs. 3(a) and 3(b) for copper. We have used for the frequencies of the phonons the reduced quantity Ω given by the equation

$$\Omega^2=\omega^2 M_M/2\alpha_{MM} \quad ,$$

where ω is the actual frequency of the phonon and M_M is the mass of a bulk atom.

In the low-energy range the validity of the central-force approximation can be tested on the elastic constants of the material. In this model, we have the following relations:

$$C_{11}=2\alpha_{MM}/a\,, \quad C_{44}=C_{12}=\alpha_{MM}/a \quad .$$

In the case of the nickel, with $\alpha_{\mathrm{Ni\,Ni}}=3.79\times10^4$ dyn/cm, the calculated elastic constants are, respectively, 13, 12, and 28% different from the experimental data.[19] In the case of copper, the force constant has been adjusted to the maximum frequency: $\alpha_{\mathrm{Cu\,Cu}}=2.72\times10^4$ dyn/cm. The calculated elastic constants C_{11}, C_{44}, and C_{12} are 11, 1, and 38% different from the experimental data.[21] From a general point of view, considering the above relations between α_{MM}, C_{11}, C_{44}, and C_{12}, a necessary condition for the validity of the central-force model is $C_{11}\simeq 2C_{44}$. From the experimental data, one can see that only nickel and copper in fcc crystals and iron in bcc crystals fit this condition.

If we than adopt the approximation of the central forces between nearest neighbors, in the case of a

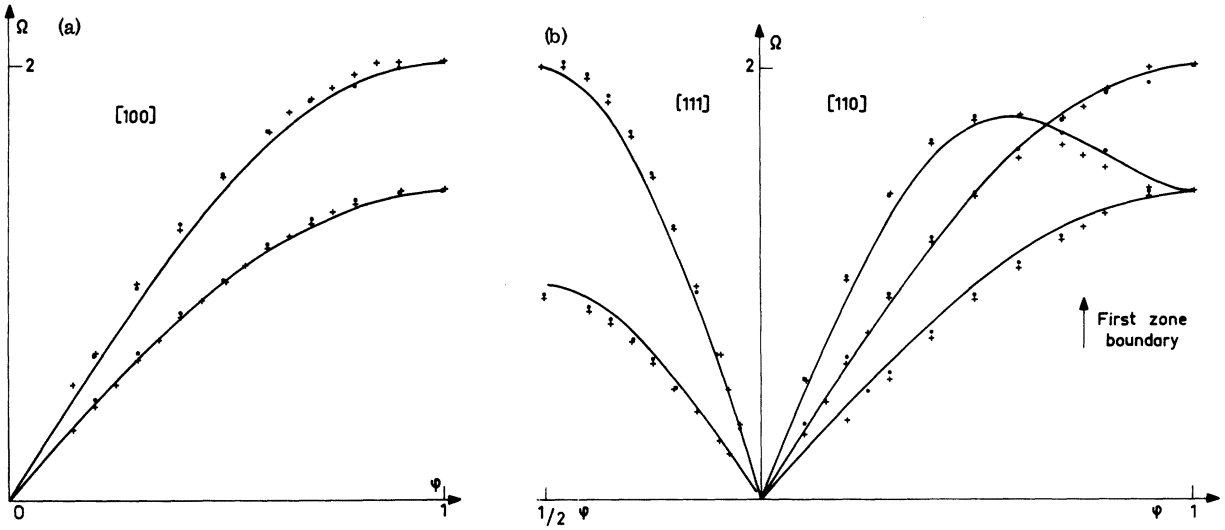

FIG. 3. Comparison between the experimental dispersion curves [Nicklow *et al.* (Ref. 20)] and the calculated ones (in the approximation of central forces between nearest neighbors) for copper. We have used for the frequencies the reduced quantity Ω (see the text). The reduced wave vector φ is given by the equation $\varphi = ka/\pi$, where a is the lattice constant. (a) Waves propagating along the [100] direction; (b) waves propagating along the [110] and [111] directions.

$C(2\times2)$R adsorbed layer, we will have to take into account the following force constants: α_{AB} between type A and B atoms, and, in the same notation, α_{AA}, α_{BB}, α_{AM}, α_{BM}. By referring these constants to the bulk constants, we finally get the following reduced set of parameters:

reduced masses

$$\mu_A = M_A/M_M, \quad \mu_B = M_B/M_M \ ;$$

reduced force constants

$$\beta_{AM} = \alpha_{AM}/\alpha_{MM}, \quad \beta_{AB} = \alpha_{AB}/\alpha_{MM}, \quad \beta_{BM} = \alpha_{BM}/\alpha_{MM} \ ,$$

$$\beta_{AA} = \alpha_{AA}/\alpha_{MM}, \quad \beta_{BB} = \alpha_{BB}/\alpha_{MM} \ .$$

It must be noted that β_{AA} and β_{BB} are next-nearest-neighbors force constants in the sense of the bulk distances, and should be neglected in our nearest-neighbor approximation. Nevertheless, these constants are necessary to describe the bonds in the adsorbate plane, especially in the case of $C(2\times2)$NR (suppression of B), where β_{AA} remains the only force constant in the adsorbate plane.

III. GENERAL PROPERTIES OF THE MODEL

From the symmetry of the crystalline structure of the model, we can deduce two general properties of the atomic vibrations, which are independent of the force-constant model adopted.

First, the crystal has the "axial inversion symmetry"[22] (each atom lies on an axis, normal to the surface, such that a rotation of 180° about this axis carries every atom in the crystal into a position formerly occupied by an equivalent atom). This implies[22] that the displacements of each atom, for a given vibration mode, are situated on an ellipse which has one axis perpendicular to the surface and the other parallel to the surface. Furthermore, the plane containing the normal to the [001] surface (i.e., the [001] axis) and the [100] axis is a "complete reflection symmetry" plane[22] (a reflection through this plane carries every atom in a position which was formerly occupied by an equivalent atom). This implies[22] a "partitioning" into two classes for the surface modes with a wave vector (k_x, k_y) parallel to this plane: one class of modes polarized in the sagittal plane, i.e., the plane containing the [001] and [100] axis (two-thirds of the modes) and another class of modes polarized along the [010] axis, i.e., of pure shear-horizontal waves (one-third of the modes). The same property is found for the [110] direction in the $P(1\times1)$ case.

Another important property of our model is related to the type of interactions retained for describing the elastic energy of the crystal. In this central-force approximation, as the elastic energy depends only on the relative distance between nearest neighbors, the expression is unaffected by a rotation of the crystal as a whole. In other words, the force-constant model has rotational invariance, which is a necessary condition for obtaining the correct dispersion relations in the long-wavelength region.[11] This rotational invariance is obtained whatever the masses and the force constants are in the surface region.

Finally, the maximum number of surface modes can be determined for each case of surface crys-

talline structure. In the case of $P(1\times1)$ monolayer, if N is the number of atoms in a (001) plane, $2N$ atoms (plane $n=0$ and $n+1$) have a neighborhood (in the sense of nearest neighbors) distinct from a bulk atom neighborhood.

Consequently, $3\times2N$ surface phonons will appear. This will correspond to six branches of surface modes in the Brillouin zone. It must be noted that this number is an upper limit of the number of surface branches. In fact, for a given set of parameters, some of the surface branches can be located inside the bulk bands. In this case, they correspond to virtual surface modes. As already discussed above, the $C(2\times2)$R structure will have twice as many branches as the $P(1\times1)$ structure. The maximum number of surface branches in the $C(2\times2)$R structure will be 12 associated with four types of atoms (A, B, C, D) distinct from the bulk atoms. In the $C(2\times2)$NR case, three types of atoms (A, C, D) remain, corresponding to a maximum of nine surfaces branches, divided into real and virtual surface modes for a given set of parameters.

IV. EQUATIONS AND METHOD OF CALCULATION

A. Two types of bulk atoms

Before developing the equations, it is necessary to examine in detail the distinction introduced by type-A and type-B atoms between the substrate atoms. Let us consider the plane $n=1$. One type-C atom has two A atoms and two B atoms as nearest neighbors. The interactions involved with the A atoms are directed in the plane defined by the [100] and [001] directions, associated with the force constant α_{AM}. The interactions involved with the B atoms are directed in the plane defined by [010] and [001] direction, associated with the force constant α_{BM}. In the case of D atoms, the roles of A and B are exchanged. It is to be noted that type C and type D build up a $C(2\times2)$R lattice which can be formed by translation from the adsorbate plane. One possible translation, which carries A onto C and B onto D, corresponds to the vector

$$\hat{t}=\tfrac{1}{2}a\,\hat{x}+\tfrac{1}{2}a\,\hat{z}\quad.$$

$\hat{z}$ is directed towards the inside of the crystal.

The same considerations can be applied to the atoms of the plane $n=2$ where we have also two types of atoms C and D obtained from the C and D atoms of the plane $n=1$ through a translation of $\hat{t}$.

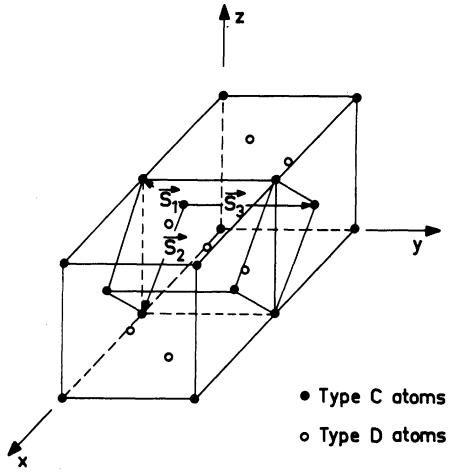

FIG. 4. Bulk unit cell for the fcc crystal in the case when the two types of atoms C and D are distinguished.

Then, from plane to plane, the distinction applies to every bulk atom. The crystal must be divided into two sublattices C and D. As these sublattices are built up by means of $\hat{t}$, the atoms of one type are contained in planes parallel to $\hat{t}$, i.e., in the (010) planes, two adjacent planes containing atoms of different types. This is illustrated in Fig. 4. The unit cell for the sublattice of type C atoms is shown in Fig. 4. It is built up on the vectors $\vec{S}_1$, $\vec{S}_2$, $\vec{S}_3$ and is a rectangular prism.

A quarter of the corresponding Brillouin zone [a rectangular prism with the following dimensions: $(\sqrt{2}\,2\pi/a,\ \sqrt{2}\,2\pi/a,\ 2\pi/a)$] is shown in Fig. 5 inserted in the Brillouin zone of the nondifferentiated crystal.

B. Equations of the movement

Since the interactions are limited to the nearest neighbors the atoms in the planes $n\geq2$ are "bulk" atoms. The atomic displacements in the bulk and at the surface are then described by the following set of equations: (i) six equations for the plane $n=0$ (type-A and type-B atoms); (ii) six equations for the plane $n=1$ (type-C and type-D atoms). (iii) six equations for the planes $n=2$ (type-C and type-D atoms). If u^j, v^j, w^j, denote the displacements of a type j atom along x, y, and z and if l, m, n label the equilibrium position of this atom with respect to x, y, z, the equations have the following form:

for the type-A atoms:

$$\mu_A(M_M/\alpha_{MM})\ddot{u}^A_{l,m,0}=\beta_{AA}(u^A_{l+2,m,0}+u^A_{l-2,m,0}-2u^A_{l,m,0})+\tfrac{1}{2}\beta_{AB}(u^B_{l+1,m+1,0}+u^B_{l-1,m-1,0}+u^B_{l-1,m-1,0}+u^B_{l+1,m-1,0}-4u^A_{l,m,0}$$

$$+v^B_{l+1,m+1,0}-v^B_{l+1,m-1,0}+v^B_{l-1,m-1,0}-v^B_{l-1,m+1,0})+\tfrac{1}{2}\beta_{AM}[u^C_{l+1,m,-1}+u^C_{l-1,m,-1}-2u^A_{l,m,0}$$

$$+ w^C_{l+1,m,1} - w^C_{l-1,m,1}] \quad , \tag{1}$$

$$\mu_A\,(M_M/\alpha_{MM})\,\ddot{v}^A_{l,m,0} = [\text{Eq. (1) with } u \rightarrow v,\ l \rightarrow m,\ C \rightarrow D] \quad , \tag{2}$$

$$\mu_A\,(M_M/\alpha_{MM})\,\ddot{w}^A_{l,m,0} = \tfrac{1}{2}\,\beta_{AM}\,(w^C_{l+1,m,1} + w^D_{l,m+1,1} + w^C_{l-1,m,1} + w^D_{l,m-1,1} - 4\,w^A_{l,m,0} + u^C_{l+1,m,1} - u^C_{l-1,m,1} + v^D_{l,m+1,1} - v^D_{l,m-1,1}) \quad , \tag{3}$$

$$\ddot{u}_B = [\text{Eq. (1) with } A \rightarrow B,\ C \rightarrow D] \quad , \tag{4}$$

$$\ddot{v}_B = [\text{Eq. (2) with } A \rightarrow B,\ C \rightarrow D] \quad , \tag{5}$$

$$\ddot{w}_B = [\text{Eq. (3) with } A \rightarrow B,\ C \rightarrow D] \quad ; \tag{6}$$

for type-C atoms in the plane $n = 1$:

$$(M_M/\alpha_{MM})\,\ddot{u}^C_{l,m,1} = \tfrac{1}{2}\,\beta_{AM}\,(u^A_{l+1,m,0} + u^A_{l-1,m,0} - 2\,u^C_{l,m,1} + w^A_{l-1,m,0} - w^A_{l+1,m,0}) + \tfrac{1}{2}\,(u^D_{l+1,m+1,1} + u^D_{l-1,m+1,1} + u^D_{l-1,m-1,1} + u^D_{l+1,m-1,1} + u^C_{l+1,m,2} + u^C_{l-1,m,2} - 6\,u^C_{l,m,1} + v^D_{l+1,m+1,1} - v^D_{l+1,m-1,1} + v^D_{l-1,m-1,1} - v^D_{l-1,m+1,1} + w^C_{l+1,m,2} - w^C_{l-1,m,2}) \quad , \tag{7}$$

$$(M_M/\alpha_{MM})\,\ddot{v}^C_{l,m,1} = \tfrac{1}{2}\,\beta_{BM}\,(v^B_{l,m+1,0} + v^B_{l,m-1,0} - 2\,v^C_{l,m,1} + w^B_{l,m-1,0} - w^B_{l,m+1,0}) + \tfrac{1}{2}\,(v^D_{l+1,m+1,1} + v^D_{l+1,m-1,1} + v^D_{l-1,m-1,1} + v^D_{l-1,m+1,1} + v^D_{l,m+1,2} + v^D_{l,m-1,2} - 6\,v^C_{l,m,1} + u^D_{l+1,m+1,1} - u^D_{l+1,m-1,1} + u^D_{l-1,m-1,1} - u^D_{l-1,m+1,1} + w^D_{l,m+1,2} - w^D_{l,m-1,2}) \quad , \tag{8}$$

$$(M_M/\alpha_{MM})\,\ddot{w}^C_{l,m,1} = \tfrac{1}{2}\,\beta_{AM}\,(w^A_{l+1,m,0} + w^A_{l-1,m,0} - 2\,w^C_{l,m,1} + u^A_{l-1,m,0} - u^A_{l+1,m,0}) + \tfrac{1}{2}\,\beta_{BM}\,(w^B_{l,m+1,0} + w^B_{l,m-1,0} - 2\,w^C_{l,m,1} + v^B_{l,m-1,0} - v^B_{l,m+1,0}) + \tfrac{1}{2}\,(w^C_{l+1,m,2} + w^C_{l-1,m,2} + w^D_{l,m+1,2} + w^D_{l,m-1,2} - 4\,w^D_{l,m,1} + u^C_{l+1,m,2} - u^C_{l-1,m,2} + v^D_{l,m+1,2} - v^D_{l,m-1,2}) \quad ; \tag{9}$$

for type-D atoms on the plane $n = 1$:

$$\ddot{u}_D = [\text{Eq. (7) with } A \rightarrow B,\ C \rightarrow D] \quad , \tag{10}$$

$$\ddot{v}_D = [\text{Eq. (8) with } A \rightarrow B,\ C \rightarrow D] \quad , \tag{11}$$

$$\ddot{w}_D = [\text{Eq. (9) with } A \rightarrow B,\ C \rightarrow D] \quad ; \tag{12}$$

for type-C atoms on the planes $n \geq 2$:

$$\ddot{u}_C = [\text{Eq. (7) with } A \rightarrow C,\ B \rightarrow D,\ \beta = 1] \quad , \tag{13}$$

$$\ddot{v}_C = [\text{Eq. (8) with } A \rightarrow C,\ B \rightarrow D,\ \beta = 1] \quad , \tag{14}$$

$$\ddot{w}_C = [\text{Eq. (9) with } A \rightarrow C,\ B \rightarrow D,\ \beta = 1] \quad ; \tag{15}$$

for type-D atoms in the planes $n \geq 2$:

$$\ddot{u}_D = [\text{Eq. (10) with } A \rightarrow C,\ B \rightarrow D,\ \beta = 1] \quad , \tag{16}$$

$$\ddot{v}_D = [\text{Eq. (11) with } A \rightarrow C,\ B \rightarrow D,\ \beta = 1] \quad , \tag{17}$$

$$\ddot{w}_D = [\text{Eq. (12) with } A \rightarrow C,\ B \rightarrow D,\ \beta = 1] \quad . \tag{18}$$

If we try for the displacement field the following solution:

$$(u^j_{l,m,n},\ v^j_{l,m,n},\ w^j_{l,m,n}) = (U^j,\ V^j,\ W^j)\exp i\,[\tfrac{1}{2}\,k_x\,la + \tfrac{1}{2}\,k_y\,ma + \tfrac{1}{2}\,k_z\,na - \omega t] \quad ,$$

the bulk equations [(13)–(18)] reduce to the matrix system

$$\begin{pmatrix} A & B \\ B & A \end{pmatrix} \begin{pmatrix} d^C \\ d^D \end{pmatrix} = 0 \quad ,$$

with

$$A = \begin{pmatrix} \Omega^2 - 2 + \cos\varphi_x \cos\varphi_z & 0 & -\sin\varphi_x \sin\varphi_z \\ 0 & \Omega^2 - 2 & 0 \\ -\sin\varphi_x \sin\varphi_z & 0 & \Omega^2 - 2 + \cos\varphi_x \cos\varphi_z \end{pmatrix} \quad ,$$

$$B=\begin{pmatrix} \cos\varphi_x\cos\varphi_y & -\sin\varphi_x\sin\varphi_y & 0 \\ -\sin\varphi_x\sin\varphi_y & \cos\varphi_x\cos\varphi_y+\cos\varphi_y\cos\varphi_z & -\sin\varphi_y\sin\varphi_z \\ 0 & -\sin\varphi_y\sin\varphi_z & \cos\varphi_y\cos\varphi_z \end{pmatrix} ,$$

$$d^j=\begin{pmatrix} U^j \\ V^j \\ W^j \end{pmatrix} , \quad j=C \text{ or } D ,$$

$\Omega^2=\omega^2 M_M/2\alpha_{MM}$, $\varphi_r=\frac{1}{2}k_r a$, with $r=x, y, z$.

With the appropriate change of basis

$$d_S=(1/\sqrt{2})(d^C+d^D), \quad d_{AS}=(1/\sqrt{2})(d^C-d^D),$$

the matrix system becomes

$$\begin{pmatrix} A+B & 0 \\ 0 & A-B \end{pmatrix}\begin{pmatrix} d_S \\ d_{AS} \end{pmatrix}=0 ,$$

which becomes

$$\{D_S\, d_S=0 , \quad D_{AS}\, d_{AS}=0\} , \quad \text{with } D_S=A+B, \; D_{AS}=A-B . \tag{19}$$

It must be noted that D_S is identical to the dynamical matrix D of the nondifferentiated crystal (where type-C and type-D atoms are identical). The first equation $D_S d_S=0$ gives then the eigenvalues and eigenvectors of D in the first Brillouin zone of the differentiated crystal. On the other hand, it must be noted that

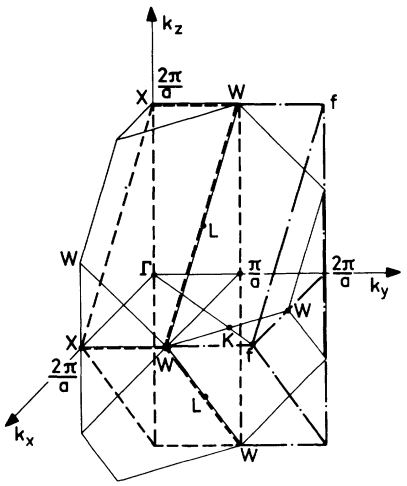

FIG. 5. Brillouin zones associated with the two types of bulk unit cell. Solid line is part of the first Brillouin zone of the fcc crystal. Dashed line is same part of the first Brillouin zone in the case of the distinction between C and D atoms, i. e., when the unit cell is the one given in Fig. 4. Dot-dashed line is part of the second Brillouin zone in the case of a distinction between C and D atoms.

$$\det\,|\,D_{AS}(\varphi_y)\,|=\det\,|\,D_S(\pi-\varphi_y)\,| \quad .$$

The second equation $D_{AS}d_{AS}=0$ gives then the eigenvalues and eigenvectors of D in the second Brillouin zone of the differentiated crystal. As it is shown in Fig. 5, the ensemble of the first and second Brillouin zone of the differentiated crystal is effectively equivalent, through the appropriate symmetries (rotation of 180° around the WLW axis) to the first Brillouin zone of the nondifferentiated crystal. Every eigenvalue and eigenvector of D is then effectively given by the system of equations.[19]

By setting $(\varphi_{S,p}, \eta_{S,p}, \lambda_{S,p})$ as the components of d_S solution of the matrix equation $D_S d_S=0$ (p being the band index) for a given set of (Ω, k_x, k_y) and $(\varphi_{S,p}, \eta_{S,p}, \lambda_{S,p})$ as the components of d_{AS} solutions of the matrix equation $D_{AS}d_{AS}=0$ under the same conditions, the atomic displacements take the following form:

$$(u^C, v^C, w^C) = \sum_{p=1}^{3}[K_{S,p}(\varphi_{S,p}, \eta_{S,p}, \lambda_{S,p})\exp i\phi_{S,p} + K_{AS,p}(\varphi_{AS,p}, \eta_{AS,p}, \lambda_{AS,p})\exp i\phi_{AS,p}], \tag{20}$$

$$(u^D, v^D, w^D) = \sum_{p=1}^{3}[K_{S,p}(\varphi_{S,p}, \eta_{S,p}, \lambda_{S,p})\exp i\phi_{S,p} - K_{AS,p}(\varphi_{AS,p}, \eta_{AS,p}, \lambda_{AS,p})\exp i\phi_{AS,p}], \tag{21}$$

with

$$\phi_{S,p} = i(\varphi_x l + \varphi_y m + \varphi_{zS,p} n - \omega t) \quad ,$$

$$\phi_{AS,p} = i(\varphi_x l + \varphi_y m + \varphi_{zAS,p} n - \omega t) \quad .$$

For a given set of (Ω, k_x, k_y) the system (19) becomes an equation in φ_z. If φ_z is real, the displacement field corresponds to a bulk phonon. If φ_z is complex, Ω falls outside the bulk bands. We can set $e^{i\varphi_z n} = e^{-nq}$, with q real or complex.

Following the nature of q, the displacement field can be a Rayleigh, alternating Rayleigh, or generalized Rayleigh wave as discussed in Sec. I. For getting a real surface wave, it is necessary for the six solutions of (19) [$q_{S,p}$ and $q_{AS,p}$ with ($p = 1, 2, 3$)] to be simultaneously distinct from a purely imaginary number, otherwise we obtain a virtual surface wave.

C. Boundary conditions—method of calculation

Assume that, for a given set of (Ω, k_x, k_y), the system (19) gives a real surface wave with six values $q_{S,p}$ and $q_{AS,p}$ distinct from a purely imaginary number. This surface will exist in the crystal if the displacement field, given by (20) and (21), satisfies the boundary conditions, i.e., Eqs. (1)–(12). In other words, a solution of (1)–(12) must have the form

$$(u^C, v^C, w^C)_{l,m,1} = (e^{\phi}) \left(\sum_{p=1}^{3} [K_{S,p}(\varphi_{S,p}, \eta_{S,p}, \lambda_{S,p}) \exp(-q_{S,p}) + K_{AS,p}(\varphi_{AS,p}, \eta_{AS,p}, \lambda_{AS,p}) \exp(-q_{AS,p})] \right), \tag{22}$$

$$(u^D, v^D, w^D)_{l,m,1} = (e^{\phi}) \left(\sum_{p=1}^{3} [K_{S,p}(\varphi_{S,p}, \eta_{S,p}, \lambda_{S,p}) \exp(-q_{S,p}) - K_{AS,p}(\varphi_{AS,p}, \eta_{AS,p}, \lambda_{AS,p}) \exp(-q_{AS,p})] \right) , \tag{23}$$

with

$$\phi = i(\varphi_x l + \varphi_y m - \omega t) \quad ,$$

$$(u^A, v^A, w^A)_{l,m,0} = (e^{\phi}) \left(\sum_{p=1}^{3} J_{S,p}(\varphi_{S,p}, \eta_{S,p}, \lambda_{S,p}) + J_{AS,p}(\varphi_{AS,p}, \eta_{AS,p}, \lambda_{AS,p}) \right) , \tag{24}$$

$$(u^B, v^B, w^B)_{l,m,0} = (e^{\phi}) \left(\sum_{p=1}^{3} J_{S,p}(\varphi_{S,p}, \eta_{S,p}, \lambda_{S,p}) - J_{AS,p}(\varphi_{AS,p}, \eta_{AS,p}, \lambda_{AS,p}) \right) . \tag{25}$$

By transporting Eqs. (22)–(25) into (1)–(12), we finally obtain a linear homogen system of 12 equations with 12 unknowns ($J_{S,p}$, $J_{AS,p}$, $K_{S,p}$, $K_{AS,p}$, $p = 1, 2, 3$). The determinant Δ of this system must be null for getting the compatibility of the surface wave with the boundary conditions.

The method of calculation consists then in the following steps: at a given set of (k_x, k_y), Ω is varied from 0 up to a certain maximum in relative increments of 10^{-3}; for each set of values one calculates Δ; when Δ vanishes, the set (k_x, k_y, $q_{S,p}$, $q_{AS,p}$) characterizes a real surface wave. Due to the size of Δ and the small increment necessary, a full exploration in Ω for a given set of (k_x, k_y) requires approximately 30 sec on a IBM 360-91 computer in the case of a $C(2\times2)$R structure.

In the case of a $C(2\times2)$NR, one has to set $\beta_{BB} = \beta_{AB} = \beta_{BM} = 0$ and to impose $u^B = v^B = w^B = 0$. This last condition leads to three linear relations between $J_{S,p}$ and $J_{AS,p}$, which, with the nine remaining equations of movement, still give a 12×12 system for Δ.

From (22)–(25) it is clear that the maximum amplitude for the displacements lies in the planes $n = 0$ or $n = 1$. This is due to the nearest neighbors approximation we have retained. In a longer-range forces model, this maximum could be situated deeper into the crystal, as mentioned by Allen, Alldredge, and de Wette.[10]

V. RESULTS AND DISCUSSION

As already discussed in Sec. III, in the [100] direction ($k_y = 0$, $0 \le k_x < 2\pi/a$) the bulk and surface modes are divided into two classes: one-third of the modes are transverse modes (hereafter denoted Y modes), i.e., with a polarization in the [010] direction; two-thirds of the modes are mixed modes (hereafter denoted XZ modes), i.e., with a polarization in the (010) plane. The system $\{D_S d_S = 0$ $D_{AS} d_{AS} = 0\}$ reduces to two equations of the first degree and two equations of the second degree in Ω. The determinant Δ separates into a 4×4 and a 8×8 determinant. It must be noted that such a differentiation into Y and XZ modes offers an important experimental interest since the "probe" particle (photon or electron) can be sensitive to the polarization of the surface modes.

We shall therefore in full detail, the case of the surface phonons propagating in the [100] direction for the various structures. Some preliminary results have already been published.[23]

A. $P(1 \times 1)$ structure

We shall discuss upon the influence of the various parameters on the dispersion curves of the surface phonons. As A and B are identical in this structure, there remains only three parameters: (i) the relative mass μ_A of the adsorbed atoms, (ii) the relative central force constant β_{AA} between nearest neighbors in the adsorbate plane; and (iii)

TABLE I. $P(1\times1)$ structure. Computed cases for the study of the influence of the mass of the adsorbed atom ($\beta_{AM}=\beta_{AA}=1$, $\beta'_{AA}=0$).

Value of μ_A	Notation	Physical situation
1	CS	clean-surface case
2	1	heavy-atom case
0.5	2	light-atom case
0.25	3	light-atom case
0.1	4	light-atom case

the relative central force constant β_{AM} between an adsorbed atom and its nearest neighbors substrate atoms (situated in the plane $n=1$). A supplementary parameter β'_{AA} will also be introduced for comparison with the other structures. It is the relative central force constant between next-nearest neighbors in the adsorbate plane. In the $C(2\times2)$R case β'_{AA} will become β_{AA}, the central force constant between nearest-neighbors atoms of the same type in the adsorbate plane, while β_{AA} will become β_{AB}.

Tables I and II present the various sets of parameters for which we have computed the energies of the surface modes.

In Table I, while keeping the force constants as in the bulk

$$\beta_{AM}=\beta_{AA}=1\ ,\quad \beta'_{AA}=0\ ,$$

we have varied the mass of the adsorbed atoms.

In Table II, restricting to a typical case ($\mu_A=0.5$) we have changed the force constants.

1. General remarks

The results are shown in Figs. 6–10. In Fig. 6, one can see the bulk bands corresponding to ($k_y=0$, $0\leq k_x<2\pi/a$). The maximum frequency for bulk phonons is $\Omega_{max}=2$. As discussed in Sec. IV, the *real* surface phonons exist only if they are situated outside of the bulk bands. In fact, due to the partitioning into X and XZ modes for the bulk and surface modes, the phonons of one class of modes are

TABLE II. $P(1\times1)$ structure. Computed cases for the study of the influence of the force constants ($\mu_A=0.5$).

Value of β_{AM}	Value of β_{AA}	Value of β'_{AA}	Notation	Physical situation
1	2	0	5	influence of β_{AA}
2	1	0	6	influence of β_{AM}
2	2	0	7	combined influence of β_{AA} and β_{AM}
2	2	1	8	combined influence of every β

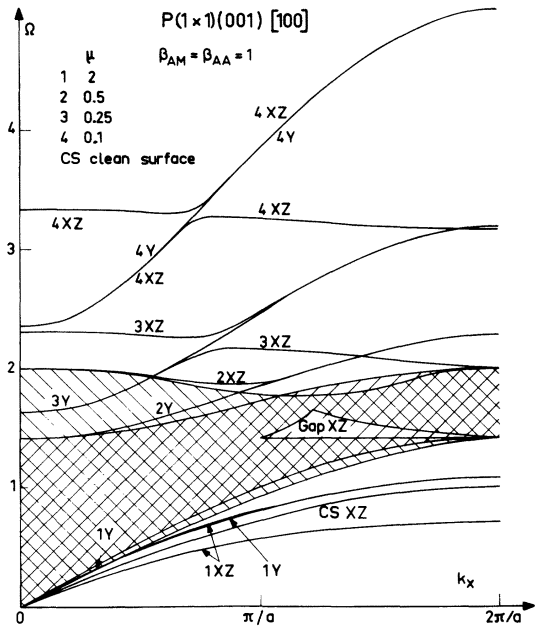

FIG. 6. Influence of the mass of the adsorbed atoms on the surface modes in the case of a $P(1\times1)$ overlayer. The various sets of parameters are defined in the figure.

orthogonal to the phonons of the other. Consequently, a surface phonon of the Y class can overlap with bulk band of the XZ class and vice versa. This particular case is observed in Fig. 6, 9, and 10.

The possible regions for the surface modes are then, as shown in Fig. 6, (i) the region under the bulk bands ("acoustical modes"), (ii) the region above the bulk bands ("optical modes"); (iii) in the case of XZ modes, an intermediate region is also possible: a "gap" in the bulk bands ("gap modes").

In order to increase the "visibility" of the results when the surface branches are very close to bulk bands we plot in Fig. 7 the difference between the acoustic XZ branch energy and the bulk band limit energy on an enhanced scale. In Fig. 8, we have focused on the gap region. As discussed in Sec. III, the maximum possible number of branches is two branches of Y modes and four branches of XZ modes. The real number of branches depends, of course, on the particular values chosen for parameters. In case 3, for instance, we have one optical Y branch (Fig. 6), two optical XZ branches (Fig. 6), one gap XZ branch (Fig. 8), no acoustical Y branch (Fig. 6), and one acoustical XZ branch (Fig. 7). We finally get four XZ branches and one Y branch in this case. In cases 6, 7, and 8, we obtain, for a very narrow range in k_x around $3\pi/2a$ (Fig. 8), five XZ branches, and one Y branch. Although the total number of six possible branches is not passed beyond, such a number of XZ branches is in disagreement with the arguments on the par-

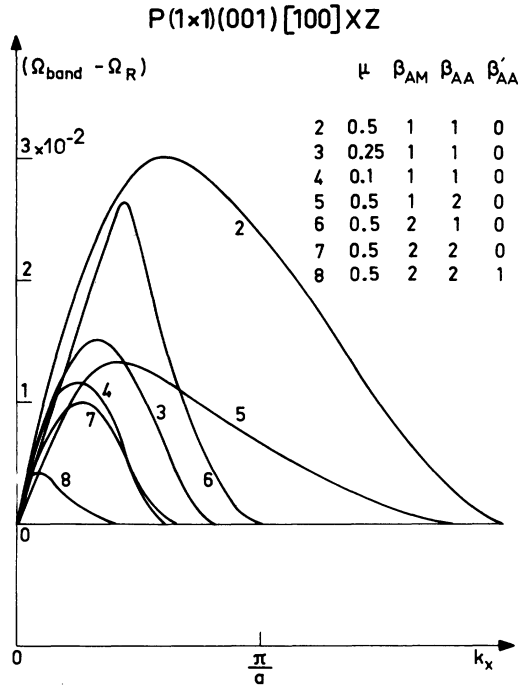

FIG. 7. Acoustical surface modes for various cases of $P(1\times1)$ overlayer. For clarity, instead of Ω, we have plotted the difference between Ω and the lower limit Ω_{band} of the bulk bands at the same k.

titioning of the modes. We have not been able to explain this disagreement, only met for a very particular set of k_x, k_y, μ's, and β's.

Before studying the influence of the various parameters, we can analyze in a general manner the types of branches which can be obtained in the various cases. The starting point is the clean surface: no Y surface mode, one acoustical XZ surface mode, and one gap XZ surface mode (Figs. 6 and 8). When the mass of the adsorbed atoms is increased, the energies of the surface modes decrease and vice versa. Consequently, no optical surface modes will be obtained with μ_A greater than unity. The number of acoustical surface modes will increase and the number of gap surface modes will decrease towards zero. This is the case 1 illustrated in Figs. 6 and 8. On the contrary, if μ_A is lower than 1 and (or) the β's are greater than 1, optical surface modes will appear. The acoustical XZ surfaces modes will be very close to the bulk bands (Fig. 7) and turn to gap XZ surface modes for large β's (Fig. 8). In fact, the optical surface modes, having a higher energy than the bulk modes can be more easily separated from them experimentally. Furthermore, the experimental cases of $C(2\times2)$ monolayers correspond to $\mu_A < 1$ and $\beta \geq 1$. Consequently, in the realistic cases, striking and experimentally interesting features will be located in the optical surface modes region. The following discussions will be mostly focussed on this region.

A qualitative explanation of the results obtained in this region can be obtained by using the following remark: the optical surface modes have a high energy; this is associated (see Appendix A) with a strong damping into the crystal. A crude approximation is to assume that the damping is so strong that the atomic motions in the plane $n=1$ are very weak with respect to the ones in the plane $n=0$. In other words u^C, v^C, w^C, u^D, v^D, w^D are negligible with respect to u^A, v^A, w^A, u^B, v^B, w^B. In this very strong damping approximation, Eqs. (1)–(3) take the following form:

$$-\mu_A \Omega^2 u^A_{l,m,0} = \beta_{AA}\,(u^A_{l+1,m+1,0} + u^A_{l-1,m+1,0} + u^A_{l-1,m-1,0} + u^A_{l+1,m-1,0} - 4u^A_{l,m,0} + v^A_{l+1,m+1,0} - v^A_{l+1,m-1,0} + v^A_{l-1,m-1,0} - v^A_{l-1,m+1,0}) + \beta_{AM}(-2u^A_{l,m,0}) \quad , \tag{1'}$$

$$-\mu_A \Omega^2 v^A_{l,m,0} = \beta_{AA}\,(v^A_{l+1,m+1,0} + v^A_{l-1,m+1,0} + v^A_{l-1,m-1,0} + v^A_{l+1,m-1,0} - 4v^A_{l,m,0} + u^A_{l+1,m+1,0} - u^A_{l-1,m+1,0} + u^A_{l-1,m-1,0} - u^A_{l+1,m-1,0}) + \beta_{AM}(-2v^A_{l,m,0}) \quad , \tag{2'}$$

$$-\mu_A \Omega^2 w^A_{l,m,0} = \beta_{AM}(-4w^A_{l,m,0}) \quad . \tag{3'}$$

For a surface wave propagating in the [100] direction

$$(u^A, v^A, w^A)_{l,m,0} = (U, V, W)\exp(ik_x x - i\omega t) \quad .$$

We finally get the system

$$\mu_A \Omega^2 U = [(4\beta_{AA} + 2\beta_{AM}) - 4\beta_{AA}\cos\varphi_x]\,U \quad , \tag{1''}$$

$$\mu_A \Omega^2 V = [(4\beta_{AA} + 2\beta_{AM}) - 4\beta_{AA}\cos\varphi_x]\,V \quad , \tag{2''}$$

$$\mu_A \Omega^2 W = (4\beta_{AM})\,W \quad . \tag{3''}$$

In other words, in this very strong damping approximation, the XZ modes separate into X modes and Z modes. The X modes are superimposed on the

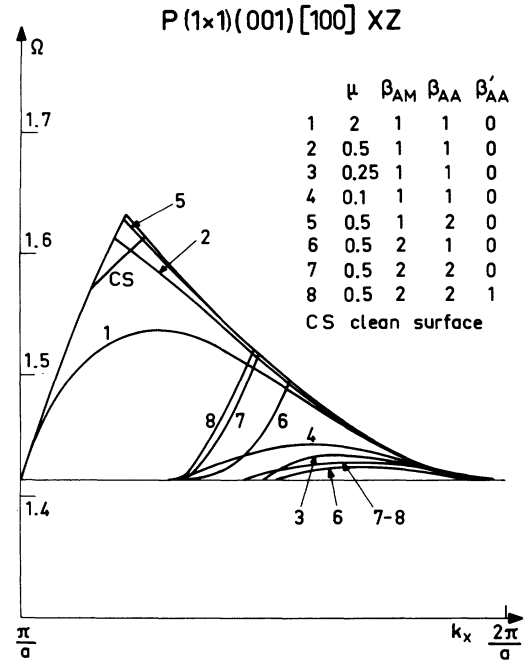

FIG. 8. Gap surface modes in the cases as in Fig. 7.

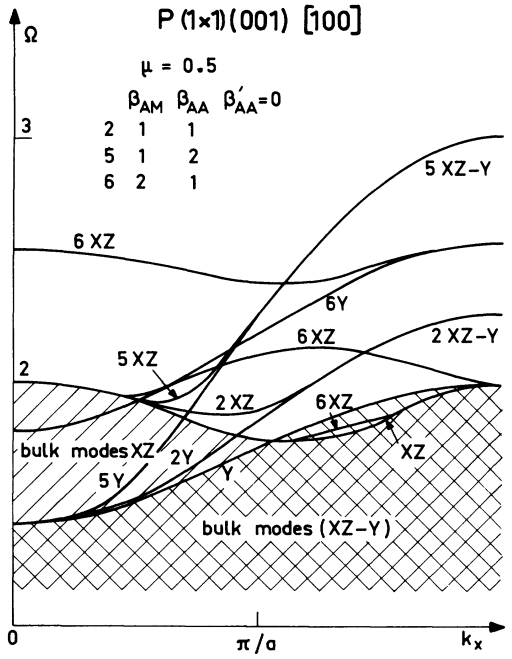

FIG. 9. Influence of the force constants β_{AM} and β_{AA} on the optical surface modes in the $P(1\times1)$ case. Bulk modes are separated in XZ and Y classes (see the text). Due to the different symmetry Y branches of surface phonons can overlap XZ bulk bands.

Y modes, their energy varies as a sinusoidal function of k_x, exhibiting a minimum for $k_x = 0$ and a maximum for $k_x = 2\pi/a$. The Z modes, on the contrary, have a constant energy independent of k_x.

The effect of a weaker damping is to couple the X and Z modes and to induce a "splitting" in the energy curves. This is schematically depicted in Fig. 11. The optical surface modes obtained in case 4 (Fig. 6), i.e., in high-energy cases where the damping is strong, have a form very similar to the one displayed in Fig. 11.

In fact, when the surface branches get closer to the bulk bands, the damping gets weaker and the "splitting" is increased between the two XZ curves.

For $k_x = 2\pi/a$ it can be shown analytically that the Z amplitude is equal to zero. As the maximum bulk frequencies are equal for Y and XZ modes the surfaces modes X and Y are symmetric. This gives a common point for this particular value of k_x.

2. *Influence of the force constants on the optical surface modes*

The influence of μ_A has just been discussed. For the following we restrict ourselves to a realistic case $\mu_A = 0.5$. In this case, for realistic values of the β's (between 1 and 3), no acoustical Y mode will be obtained and the acoustical XZ modes will be very close to the bulk bands (Fig. 7). The influence of the parameters will then be mostly visible on the optical surface modes. Case 2 ($\mu_A = 0.5$, $\beta_{AM} = \beta_{AA} = 1$, $\beta'_{AA} = 0$) can be taken as a reference;

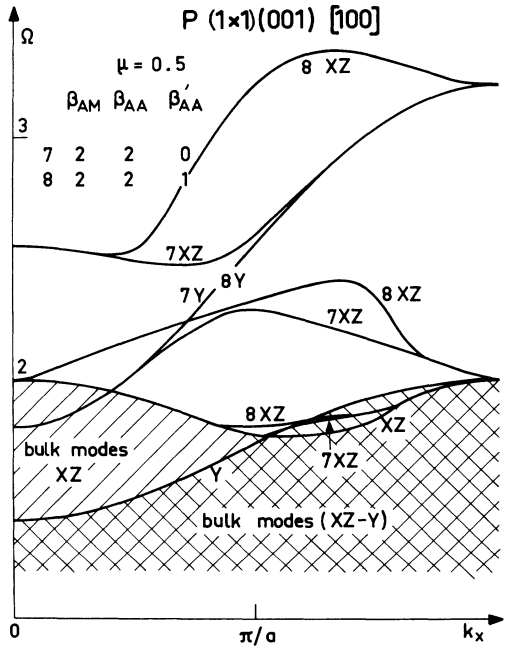

FIG. 10. Influence of the force constant β_{AA} on the optical surface modes in the $P(1\times1)$ case. See caption of Fig. 9 for the destination between bulk bands and possible overlap of surface phonons branches.

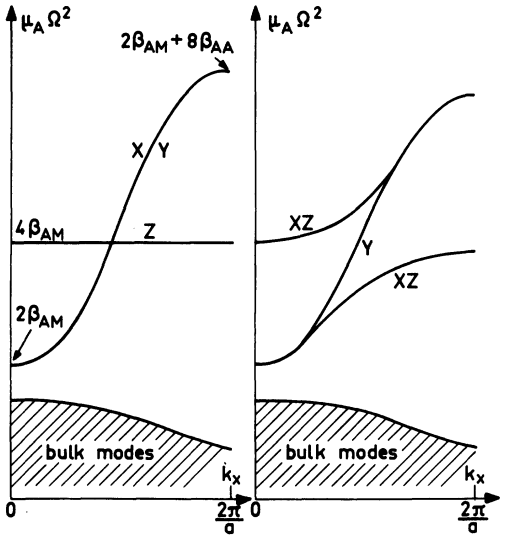

FIG. 11. Very strong damping approximation: The left-hand curves give the optical surface modes in this approximation. The right-hand curves give these modes in the approximation of weaker damping.

one gets, in this case, one optical Y branch and one optical XZ branch (the lower part of the XZ branch falls into the bulk bands).

The influence of β_{AA} can be tested by comparing cases 2 and 5 (Fig. 9). From (1''), in the very strong damping approximation the energies of the X, Y, and Z modes at $k_x = 0$ do not depend on β_{AA}. We verify in Fig. 9 that the $5Y$ and $2Y$, $5XZ$, and $2XZ$ branches are superimposed in the region of low k_x's (long wavelengths). The effect of β_{AA} is then limited to high k_x's. This can be explained in the following way: β_{AA} increases the short-range coupling between the adsorbed atoms. Its influence is then dominant on the modes of short wavelengths. We have also represented in Fig. 12 the atomic displacements associated with a Y mode at $k_x = 2\pi/a$. It is clear from the figure that β_{AA} has an influence on this Y mode.

The influence of β_{AM} can be tested by comparing the cases 2 and 6 (Fig. 9). In the very strong damping approximation, an increase of β_{AM} simply increases the energies of the optical surfaces modes without changing the shape of the branches (the sinusoidal branch keeps the same amplitude $8\beta_{AA}/\mu_A$). In Fig. 9 we verify that an increase in β_{AM} induces a general increase of the energy of any surface mode. This is due to the fact that an increase of β_{AM} reinforces the coupling between the adsorbate and the substrate. This leads to a long-range coupling increase between the adsorbed atoms via the substrate in addition to the short-range coupling increase between adsorbed and substrate atoms. Any surface mode will then be dependent on β_{AM}.

The influence of β'_{AA} can be tested by comparing the cases 7 and 8 (Fig. 10). The Y modes are not influenced (the terms in β'_{AA} vanish for the Y modes). As β'_{AA} represents the coupling between next-nearest neighbors in the adsorbed layer, the distance between these neighbors being a in the [100] direction, the surface modes having a wavelength of the order of $2a$ will correspond to antiphase motions of these neighbors and will be the most influenced. We verify in Fig. 10 that $7XZ$ and $8XZ$ branches are superimposed in the $k_x = 0$ and $k_x = 2\pi/a$ regions and strongly distinct in the $k_x = \pi/a$ region. By examining the atomic displacement associated with a XZ mode at $k_x = \pi/a$, as shown in Fig. 12, the influence of β'_{AA} is clear.

As a conclusion on the $P(1\times1)$ case, we can say that the very strong damping approximation gives a satisfactory qualitative explanation of the results. The nearest-neighbor force constants β_{AA} and β_{AM} strongly influence the energies at the optical surface modes, β_{AA}, mostly in the region $k_x = 2\pi/a$ and with a predominant effect of β_{AM} for all k_x. The next-nearest-neighbor force constant β'_{AA} modifies the energies of the surface modes mostly in the region $k_x = \pi/a$.

B. $C(2\times2)$ structures

1. *Correspondence between $P(1\times1)$ and $C(2\times2)$R*

The $P(1\times1)$ structure can be considered as a limit case of a $C(2\times2)$R structure where A and B atoms are identical ($\mu_A = \mu_B$). When $\mu_A \neq \mu_B$, the symmetry of the adsorbed monolayer and the corresponding Brillouin zone are modified. In the [100] direction the reduced zone changes from $0 \leq k_x < 2\pi/a$ to $0 \leq k_x < \pi/a$. As already discussed by Dobrzynski and Mills[12] and in this paper (Sec. II A), the introduction of new zone boundaries induces the opening of gaps in the surface-modes dispersion relations and an increase of the number of surface-mode branches by folding up of the branches in the new reduced zone. This correspondence between $P(1\times1)$ and $C(2\times2)$R is illustrated in Fig. 13. The dispersion relations of the optical-surface Y modes obtained in the $P(1\times1)$ and $C(2\times2)$R cases with the same set of force constants are plotted: $\beta_{AM} = \beta_{AB} = \beta_{BM} = 2$, $\beta_{AA} = \beta_{BB} = 0$, and with distinct masses for the adsorbed atoms $\mu_A = 0.546$, $\mu_B = 1$ for $C(2\times2)$R and $\mu_A = 0.5$ for $P(1\times1)$. If μ_A and μ_B were nearly equal with $\mu_A = 0.5$ the Y mode branch would be curve 7, which is obtained from the $P(1\times1)$ Y mode by folding up the part $k_x = \pi/a$ to $k_x = 2\pi/a$ on the part $k_x = 0$ to $k_x = \pi/a$. The differentiation of the mass μ_B opens the gap in the curve at the point $k_x = \pi/a$ and decreases the energy of the modes (μ_B is increased). This leads to curve 5, calculated for the $C(2\times2)$R

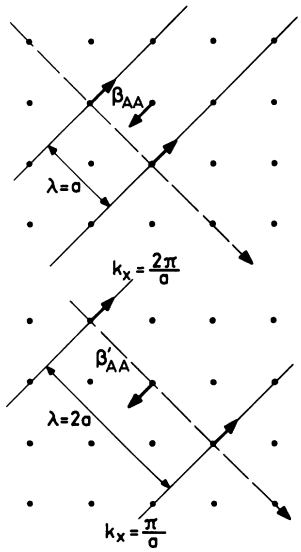

FIG. 12. Schematic explanation of the influence of β_{AA} and β'_{AA} on the surface modes. The atomic displacements associated with the optical surface modes of wave vectors π/a and $2\pi/a$ are represented. In the case $k_x=2\pi/a$, the nearest neighbors vibrate in antiphase, β_{AA} has a strong influence. In the case $k_x=\pi a$, the next-nearest neighbors vibrate in antiphase, β'_{AA} has a strong influence.

structure with $\mu_A=0.546$ and $\mu_B=1$. The same considerations, though more complicated, can be made on the XZ modes in the two structures [cases $P(1\times1)$ 8 and $C(2\times2)$ 8].

Because of this correspondence obtained by the folding up of the $P(1\times1)$ Brillouin zone, a number of properties of the $C(2\times2)$R structure can be obtained from the discussion on the $P(1\times1)$ case. An important point to notice in this folding operation is the fact that surface modes in $P(1\times1)$ structure can be mixed with the bulk bands in the case of the $C(2\times2)$R structure and then become virtual states. For instance, the gap modes of the $P(1\times1)$ case are folded up into the bulk bands in the $C(2\times2)$R case and then are no longer localized modes. Consequently, in the $C(2\times2)$R case, we can only have optical and acoustical surface modes.

From the combined effects of the folding up of the Brillouin zone and the possible mixture of surface branches and bulk bands, we verify that the maximum number of surface branches in the $C(2\times2)$R case is 12, since this number is 6 for the $P(1\times1)$ structure.

2. *Influence of the various parameters*

We have focused on the experimental case of S atoms adsorbed on Ni (100). In this case $\mu_A=0.546$ and $\mu_B=1$ [Ni atoms are combined with S atoms for building up a $C(2\times2)$R structure]. The remaining parameters are then the nearest-neighbor force constants β_{AB}, β_{AM}, β_{BM}, and the next-nearest-neighbor force constants β_{AA} and β_{BB}. The influence of β_{AB}, β_{AM}, and β_{BM} is illustrated in Fig. 14. Case 1 ($\beta_{AB}=\beta_{AM}=\beta_{BM}=1$; $\beta_{AA}=\beta_{BB}=0$) is given as a reference. We obtain one optical Y branch, one optical XZ branch, and two acoustical XZ branches. All these branches are very close to the bulk bands.

The influence of β_{AM} can be obtained by comparing case 2 ($\beta_{AM}=2$, $\beta_{AB}=\beta_{BM}=1$, $\beta_{AA}=\beta_{BB}=0$) to case 1. The increase of β_{AM} induces an increase of the energy of each surface mode. Only one acoustical XZ branch remains. The optical branches are nearly simply obtained from case 1 branches by shifting upwards. Such an influence agrees quite well with the observed influence of β_{AM} in $P(1\times1)$ case.

The influence of β_{BM} can be obtained from the comparison of the cases 4 and 5. As can be seen in Fig. 14, the difference between the surface branches in the two cases is very weak. This indicates that the B atoms (the "heavy" atoms) do not influence the surface phonons via their binding with the substrate atoms.

The influence of β_{AB} is deduced from the comparison of the cases 1 and 3. The energy of each surface mode is increased with a more pronounced effect on the modes in the $k_x=0$ region. Such an influence corresponds to the effect of β_{AA} on the

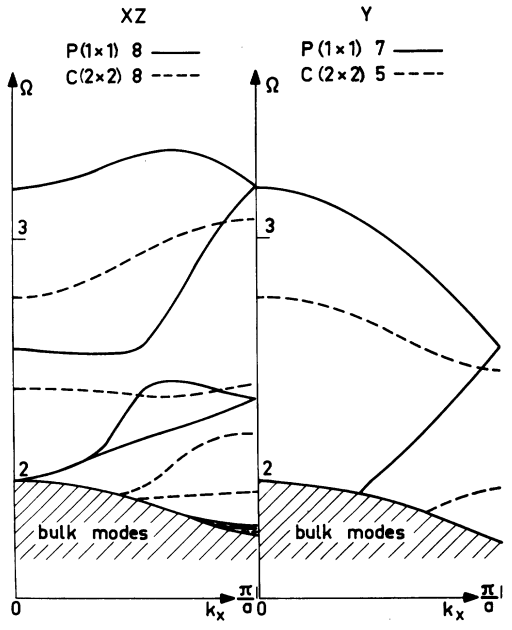

FIG. 13. Correspondence between the optical surface modes in the $P(1\times1)$ and $C(2\times2)$R structures. The force constants are the same in the two structures.

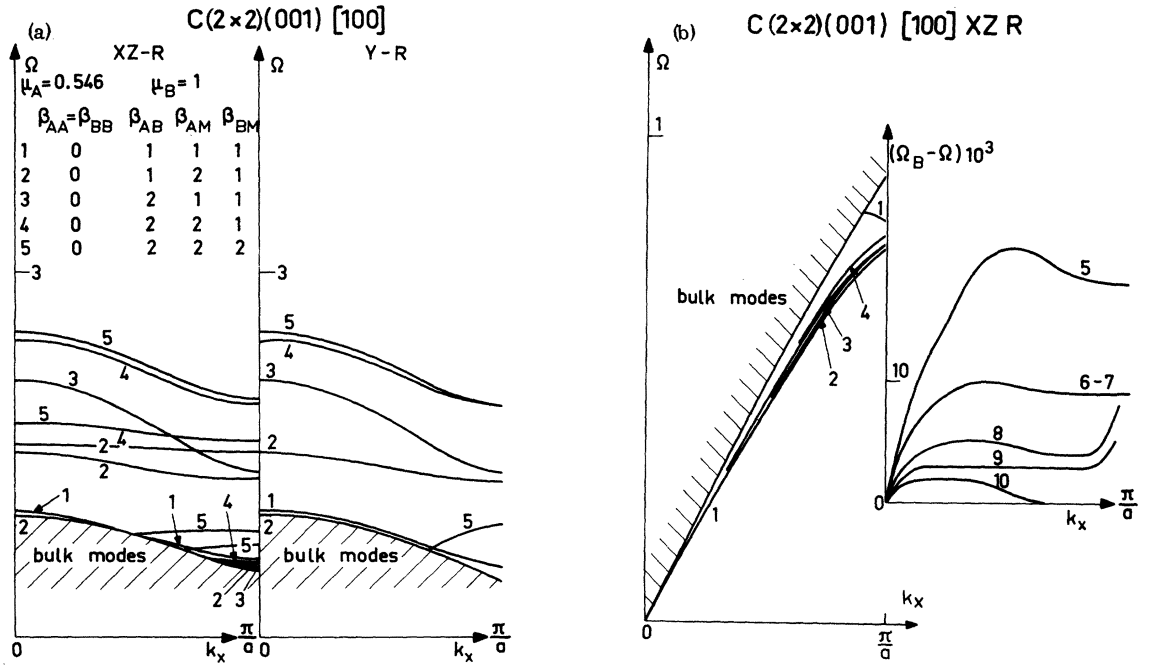

FIG. 14. (a) Optical surface modes in the $C(2\times2)$R structure for various sets of parameters. (b) Acoustical surface modes in the same cases as in Fig. (a). In addition, the cases 6–10 (meaning given in Fig. 15) are given.

modes in the $k_x = 2\pi/a$ region in the $P(1\times1)$ case, since the regions $k_x = 2\pi/a$ and $k_x = 0$ are superimposed in the $C(2\times2)$R case.

The influence of the constants AA and BB between next-nearest neighbors is given in Fig. 15. A typical influence of these force constants is observed on the highest optical XZ branches. The cases 6, 7, 8 and 9 correspond to the same points in the $k_x = 0$ region. The influence of β_{AA} and β_{BB} is only effective in the $k_x = \pi/a$ region. This is exactly the same result as for the $P(1\times1)$ case. The comparison between cases 6 and 8 indicates a very weak influence of β_{BB}, as for β_{BM}. In Fig. 15 we have only plotted the XZ branches since the Y modes are not influenced [as in $P(1\times1)$ case] by β_{AA} and β_{BB}.

As a conclusion for this $C(2\times2)$R case, we can say that the results are in clear correspondence with these for the $P(1\times1)$ structure B atoms being heavy, the force constants associated with their own motions (β_{BM} and β_{BB}) have very little influence on the surface modes. The most efficient parameter is β_{AM}, which influences each surface mode. β_{AB} is mainly efficient in the $k_x = 0$ region, while β_{AA} acts only on the $k_x = \pi/a$ region. In other words, the surface modes in the $k_x = 0$ region reflect mainly the value of the nearest-neighbor constants β_{AB} and β_{AM}. The $k_x = \pi/a$ region yields, in a complex form, some information on the next-nearest-neighbor constant β_{AA}.

C. $C(2\times2)$NR structure

Compared to the $C(2\times2)$R structure, the $C(2\times2)$ NR structure corresponds to a loosening of the bonds in the surface plane since the number of atoms in this plane is divided by 2.

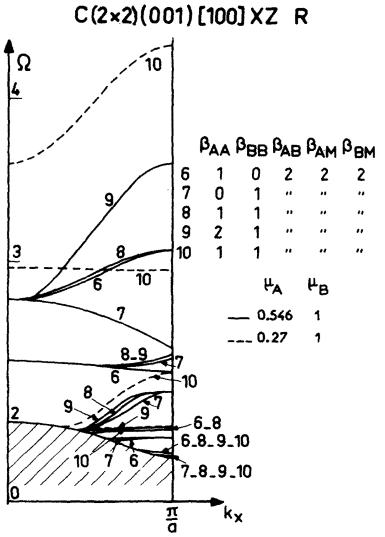

FIG. 15. Influence of the force constants β_{AA} and β_{BB} on the optical surface modes in the $C(2\times2)$R structure.

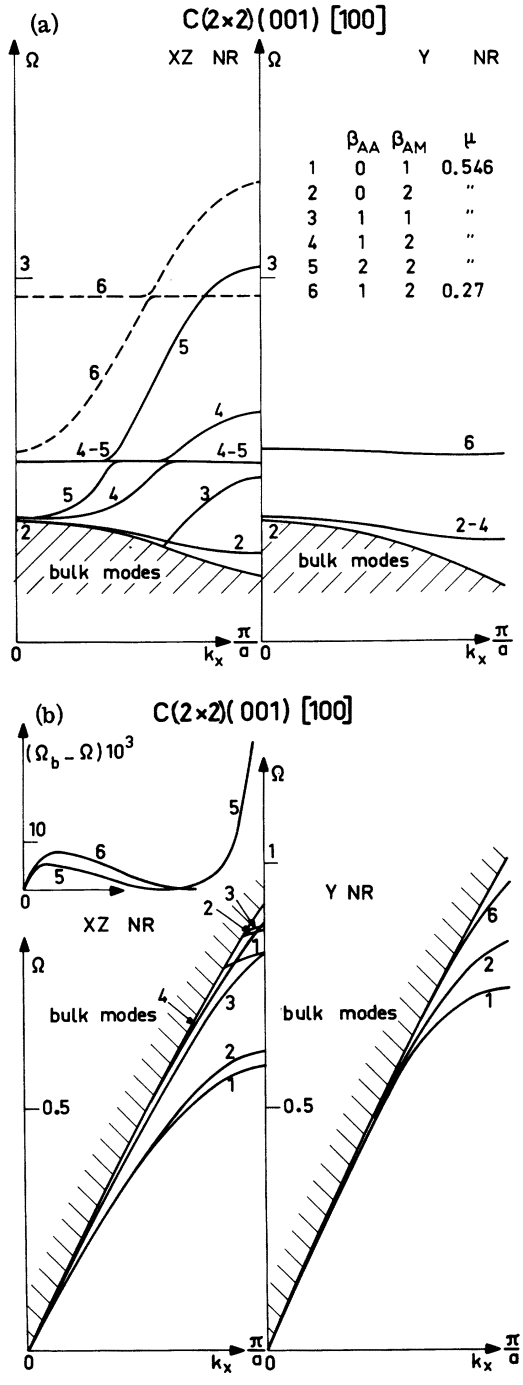

FIG. 16. Surface modes for various types of $C(2\times 2)$NR overlayers. (a) Optical surface modes; (b) acoustical surface modes.

A very general consequence will be a decrease of the energy of the surface modes. The remaining parameters are μ_A, β_{AM}, and β_{AA}. With respect to the $C(2\times 2)$R case, only one relevant parameter has been suppressed, β_{AB}. Following the above discussion we can predict that the $k_x = 0$ region will be the most affected.

The influence of the various parameters is illustrated in Fig. 16. The first major result is the appearance of new acoustical branches. This indicates a general decrease of the energy of the surface phonons. Case 1 ($\beta_{AM} = 1$, $\beta_{AA} = 0$, $\mu_A = 0.546$) is given as a reference; we obtain one acoustical Y branch, no optical Y branch, two acoustical XZ branches, and no optical XZ branch. The influence of β_{AM} is obtained from the comparison between cases 1 and 2; we observe a general increase of the energy of the surface phonons: one optical Y branch and one optical XZ branch appear, close to the bulk bands. β_{AA} has no influence on Y modes (case 2 = case 4 = case 5 and case 1 = case 3 for Y modes). Its influence of the XZ modes is obtained by comparing the cases 4 and 5; no effect in the $k_x = 0$ region, and a strong effect in the $k_x = \pi/a$ region.

As a conclusion, we can say that the force constants play the same role in the three structures. The major feature of the $C(2\times 2)$NR structure is the decrease of the energy of the surface phonons. This effect is a little more important in the $k_x = 0$ region. If we compare, for instance, the maximum frequency of the optical surface modes in the $C(2\times 2)$R and $C(2\times 2)$NR structures in the equivalent cases 8 and 4, respectively (nearest-neighbor constants equal to 2, next-nearest-neighbor constants equal to 1), we obtain for $k_x = 0$,

$\Omega_{max} = 2.76$ in the R structure ,

$\Omega_{max} = 2.24$ in the NR structure (23% lower) .

for $k_x = \pi/a$,

$\Omega_{max} = 3.08$ in the R structure ,

$\Omega_{max} = 2.46$ in the NR structure (20% lower) .

In other words, the experimental measurement of Ω_{max} would be a good test for determining whether a $C(2\times 2)$ layer is reconstructed or not.

VI. CONCLUSION

The major differences between the surface modes in the three structures are obtained in the optical surface modes region. A crude model, the very strong damping approximation, gives a good qualitative description of the dispersion relations. A correspondence between the spectra of the $P(1\times 1)$ and $C(2\times 2)$R structures has been demonstrated. For a detailed analysis of the influence of the parameters, two regions have to be considered. For $C(2\times 2)$ structures the $k_x = 0$ region gives information on the nearest-neighbors force constants and mainly on the adsorbate substrate constant β_{AM}. The $k_x = \pi/a$ region is influenced, in

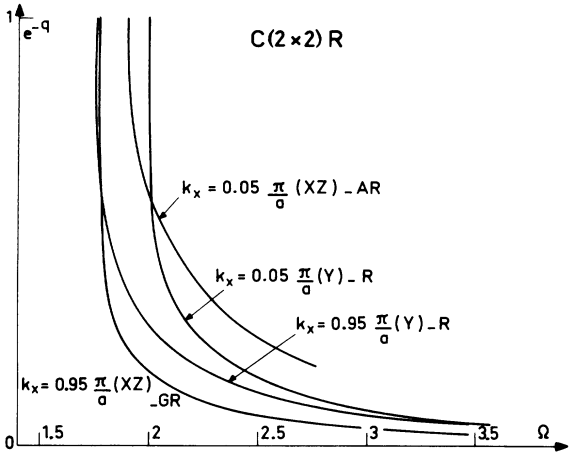

FIG. 17. Damping of the surface modes for various cases. R indicates a Rayleigh mode, AR indicates an alternated Rayleigh mode, and GR indicates a generalized Rayleigh mode.

addition, by the next-nearest-neighbor force constants between adsorbed atoms. These conclusions clearly indicate the regions of experimental interest. In particular, a measurement of the maximum frequency of the optical surface modes provides a clear out test for deciding between a $C(2\times2)$R and $C(2\times2)$NR structure.

Finally it must be noted that the method we have developed can be, in principle, extended to any type of ordered adsorbed monolayer.

ACKNOWLEDGMENTS

One of us (J. B. T.) wishes to express his gratitude to the D. R. M. E. for financial support. It is also a pleasure for us to thank Dr. L. Dobrzynski who suggested and stimulated this work. We are indebted to Y. Lejay for his great contribution in computer programming. We thank also C. Manus, D. A. Degras, and J. Lapujoulade for critical reading of the manuscript.

APPENDIX A: DAMPING OF THE SURFACE MODES

Our calculation determines not only the energy and the polarization of the surface phonons but also the value of the z component of the wave vector $\vec{k}$, i.e., $k_z = iq$. When q is real (Rayleigh-type surface mode), the value of e^{-q} represents the damping of the surface mode, when penetrating into the crystal. The lower e^{-q} the higher the damping. We have plotted the value of e^{-q} as a function of Ω for a fixed value of k_x and $k_y = 0$. This is shown in Fig. 17. It is evident from this figure that the damping increases very rapidly with Ω. Typically, for $\Omega = 2.5$, e^{-q} is of the order of 0.2. This means that the atomic motions in the plane $n = 1$ are 20% in magnitude of the atomic motions in the plane $n = 0$ and only 4% in magnitude in the plane $n = 2$. The very strong damping approximation seems then to be acceptable for $\Omega \geq 2.5$.

[1] M. A. Chester, J. Pritchard, and M. L. Sims, *Adsorption Desorption Phenomena* (Academic, New York, 1972), p. 277.
[2] J. T. Yates and D. A. King, Surf. Sci. 30, 601 (1972).
[3] H. Ibach, Phys. Rev. Lett. 24, 1416 (1970); J. Vac. Sci. Technol. 9, 713 (1972).
[4] Y. Ballu, R. A. Armstrong, and J. Lecante, C. R. Acad. Sci. Paris B 274, 718 (1972).
[5] B. R. Williams, J. Chem. Phys. 55, 3220 (1971).
[6] S. Anderson and J. B. Pendry, J. Phys. C 5, L41 (1972); F. Fortsmann, W. Berndt, and P. Buttner, Phys. Rev. Lett. 30, 17 (1973).
[7] L. Dobrzynski and D. L. Mills, J. Phys. Chem. Solids 30, 1043 (1969).
[8] P. Masri, thèses (Faculté des Sciences Orsay, France, 1971) (unpublished); P. Masri and L. Dobrzynski, J. Phys. Chem. Solids 34, 847 (1973).
[9] L. Dobrzynski, Surf. Sci. 20, 99 (1970).
[10] R. E. Allen, G. P. Alldredge, and F. W. de Wette, Phys. Rev. B 4, 1682 (1971).
[11] S. W. Musser and K. H. Riever, Phys. Rev. B 2, 3034 (1970).
[12] L. Dobrzynski and D. L. Mills, Phys. Rev. B 7, 1322 (1973).
[13] D. C. Gazis and R. F. Wallis, Surf. Sci. 5, 482 (1966).
[14] For a recent review, see, for example, G. A. Somorjai, Surf. Sci. 34, 156 (1973).
[15] See, for instance, A. U. McRae, Surf. Sci. 1, 319 (1964); for a general discussion on the problem of reconstruction, see, for example, J. W. May, Adv. Catalysis Related Subj. 21, 151 (1970).
[16] J. E. Demuth, D. W. Jepsen, and P. M. Marcus, Phys. Rev. Lett. 31, 540 (1973); S. Andersson, B. Kasemo, J. B. Pendry, and M. A. Van Hove, Phys. Rev. Lett. 31, 595 (1972).
[17] D. A. King, Le Vida 163, 51 (1973).
[18] J. de Launay, Solid State Phys. 2, 248 (1956).
[19] B. C. Clark, R. Hermann, and R. F. Wallis, Phys. Rev. 139, A860 (1965).
[20] R. M. Nicklow, G. Gilat, H. G. Smith, L. J. Raubenheimer, and M. K. Wilkinson, Phys. Rev. 164, 922 (1967); E. C. Svensson, B. N. Brockhouse, and J. M. Rowe, Phys. Rev. 155, 619 (1967).
[21] W. C. Overton and J. Gaffney, Phys. Rev. 98, 969 (1955).
[22] R. E. Allen, G. P. Alldredge, and F. W. de Wette, Phys. Rev. B 4, 1648 (1971).
[23] G. Armand and J. B. Theeten, Solid State Commun. 13, 563 (1973); Le Vida 163, 47 (1973).